

# Sampling statistics and considerations for single-shot analysis using laser-induced breakdown spectroscopy

J.E. Carranza, D.W. Hahn\*

*Department of Mechanical Engineering, University of Florida, Gainesville, FL 32611-6300, USA*

Received 10 August 2001; accepted 3 January 2002

---

## Abstract

A statistical analysis of single-shot spectral data is reported for laser-induced breakdown spectroscopy (LIBS). Fluctuations in both atomic emission and plasma continuum emission are investigated in concert for a homogenous gaseous flow, and fluctuations in plasma temperature are reported based on iron atomic emission in an aerosol-seeded flow. Threshold irradiance for plasma initiation and plasma absorption were investigated for pure gaseous and aerosol streams, with detailed statistical measurements performed as a function of pulse energy in the breakdown regime. The ratio of the analyte atomic emission intensity to the continuum emission intensity (peak/base) provided a robust signal for single-shot LIBS analysis. Moreover, at optimal temporal delay, the precision of the LIBS signal was maximized for pulse energies within the saturation regime with respect to plasma absorption of incident energy. Finally, single-shot temperature measurements were analyzed, leading to the conclusion that spatial variations in the plasma volume formation and subsequent plasma emission collection, play important roles in the overall shot-to-shot precision of the LIBS technique for gaseous and aerosol analysis. © 2002 Elsevier Science B.V. All rights reserved.

*Keywords:* Laser-induced breakdown spectroscopy (LIBS); Aerosol; Single-shot

---

## 1. Introduction

Environmental aerosols comprise a diverse and constantly fluctuating system whose behavior and properties are difficult to characterize. The United State Environmental Protection Agency (EPA) concluded in 1996 that ambient air particulate matter (notably submicron to micron-sized particles) is associated with increased morbidity and mortality [1]. Several techniques have been used

to analyze individual airborne particles in real time, including laser-induced breakdown spectroscopy. Laser-induced breakdown spectroscopy (LIBS), also known as laser-induced plasma spectroscopy, is an atomic emission spectroscopy technique that uses a laser-induced plasma as both the sample volume and the excitation source, dissociating all molecules and fine particulates within the highly energetic microplasma. The resulting plasma emission can be resolved both spectrally and temporally to yield spectra containing the atomic emission lines corresponding to the atoms present in the plasma volume, including atoms originating

---

\*Corresponding author. Tel.: +1-352-392-0807; fax: +1-352-392-1071.

*E-mail address:* dwhahn@ufl.edu (D.W. Hahn).

from within aerosols initially enveloped by the plasma. LIBS, as discussed below, is a technique that can be miniaturized, being sensitive enough for measuring aerosol elemental composition, while functioning as a real-time, in situ monitor characterized by speed and experimental simplicity.

LIBS has been applied successfully in a number of studies for the determination of overall mass concentrations, including several studies addressing continuous on-line monitoring of air emissions and aerosols [2–4]. Other research and review papers focusing on LIBS are reported in the literature [5–7]. An extension of the LIBS technique for real-time sizing and elemental analysis of single aerosol particles based on the analysis of individual LIBS spectra was reported recently [8–10]. The technique proved to be both robust and highly sensitive during initial laboratory and field measurements. The use of single-shot data analysis stands in contrast to the often-reported ensemble-averaging techniques typically used for LIBS-based analyses. While a large body of LIBS research concerning signal processing, signal optimization, and signal noise reduction has been reported based on ensemble averaging, it is not readily apparent as to applicability of this work to single-shot LIBS analysis schemes.

To date, the majority of research addressing issues to enhance LIBS sensitivity and precision is based on traditional ensemble averaging of spectra as a means to overcome the extensive spectral fluctuations observed on a laser shot-to-shot basis. Radziemski et al. studied the characteristics of laser-induced plasmas in air using generated aerosols, noting that temporal resolution was required to improve the LIBS signal, and that local thermodynamic equilibrium (LTE) was realized after approximately 1  $\mu$ s, an essential condition to obtain analytical information from the LIBS spectrum [11]. Yalcin et al. reported minimal effects due to ambient conditions such as background gas composition, the presence of aerosol particles, and humidity on the plasma under LTE, as characterized by the average plasma temperature and electron density [12]. They also found that variations in the pulse energy produced changes in the plasma temperature within the precision of the

measurements. More recent research suggests that gas matrix effects may be significant for select species such as mercury [13]. Schechter studied the problem of spectral fluctuations in LIBS analysis of aerosols using a single-shot measurement approach accompanied with a novel spectral rejection algorithm [14]. The idea was to identify single-shot spectra with the goal of rejecting anomalous events, considered spectra in which no analyte emission was present or those spectra with insufficient signal for robust analysis. Later, Schechter and co-workers developed a single-breakdown-event analysis scheme to determine absolute concentrations of elements in particulate material [15]. The approach was based on the assumption that the same fluctuation patterns observed in the analyte emission peaks were present in the baseline continuum, which were subsequently used for a data filter algorithm similar to the earlier study. Gornushkin et al. discussed a theoretical basis for considerations of atomic line-to-continuum fluctuations, with a goal of characterizing the analytical feasibility of such shot-to-shot corrections [16]. Hahn et al. developed a conditional data analysis algorithm for LIBS-based detection of individual aerosol particles that rejected spectral data based on the absence of atomic emission corresponding to the targeted analytes [9,17]. Using the conditional data analysis approach, single-shot LIBS spectra were identified and analyzed corresponding to individual particles as small as 175 nm in diameter (approx. 3 fg in mass), and aerosol mass concentration levels from low parts-per-billion to parts-per-trillion levels were recorded. Cheng also used a screening data algorithm in combination with an aerosol beam-focusing device to enhance the detection sensitivity of the LIBS technique [18].

As discussed above, the ensemble-averaging approach (including data filtering algorithms) has been widely used as a tool to overcome the often-extensive laser shot-to-shot spectral fluctuations, thereby improving the sensitivity of the LIBS technique. This approach, however, reaches a natural limit when low, to very low concentrations of aerosols comprise the analyte species of interest. Conditional data analysis algorithms applied to individual spectra (resulting in the rejection of ill-

conditioned spectra as discussed above) can improve signal-to-noise ratios, but more importantly, such conditional analysis techniques open the door to the study of single-shot LIBS spectra corresponding to individual aerosol particles. In contrast to ensemble averaging, single-shot LIBS analyses raise new questions regarding shot-to-shot fluctuations and precision. Issues of precision for LIBS-based analysis of solids, including shot-to-shot variability, were addressed in detail in a recent paper by Castle et al. [19]. However, no such studies have been reported to date with the specific application of single-shot aerosol analysis. The goal of this paper is to gain an understanding of the effects of laser pulse energy on the optimization and precision of LIBS-based single-shot analysis of gaseous and aerosol systems.

## 2. Experiment

A brief overview of the LIBS experimental set up and aerosol generation is presented here, with additional details reported previously [9,20]. The excitation source was a 1064-nm Q-switched Nd:YAG laser with a nominal pulse width of 10 ns, maximum pulse energy of 375 mJ, and operated with a 5 Hz pulse repetition rate. The laser pulse-to-pulse energy stability was  $\pm 4\%$  rms. The expanded laser beam (12-mm diameter) was focused into the sample chamber using a 75-mm UV grade plano-convex lens to create the plasma ( $f/6.25$ ). The plasma emission was collected along the incident beam in a backward direction ( $180^\circ$ ) and separated using a pierced mirror. The collected plasma emission was fiber-coupled to a 0.275-m spectrometer, dispersed with a 2400-groove/mm grating (0.03 nm/pixel, 0.12-nm resolution), and recorded with an intensified, charge-coupled device (iCCD) detector array. Aerosol streams were generated by nebulizing aqueous analyte solutions of deionized water, or of 10 000  $\mu\text{g}/\text{ml}$  of sodium or titanium in water, into a gaseous co-flow stream of either dry nitrogen or purified, dry air. Air was collected and compressed from the air-conditioned laboratory building, and then passed through a water separator, particle filter, pressure regulator, desiccant drier, and a final high-efficiency particulate (HEPA) filter prior

to entering the flow controllers and sample chamber. Nitrogen was industrial grade, compressed dry nitrogen, which was regulated and passed through a HEPA filter and flow controller prior to use.

The experimental effort was divided into four primary elements: investigation of breakdown thresholds for various conditions; plasma energy absorption; evaluation of single-shot statistical fluctuations in plasma emission; and evaluation of single-shot plasma temperature fluctuations. For the determination of laser-induced breakdown thresholds, conditional data analysis was used to calculate the percentage of laser shots generating a plasma, as based on the presence of optical emission at a delay time of 1  $\mu\text{s}$  with respect to the incident laser pulse. Plasma energy deposition was recorded using a volume absorbing calorimeter (calibrated at 1064 nm), both before and after the laser-induced plasma. Single-shot experiments were conducted primarily using the 247.86-nm carbon I atomic emission line, which originated from the presence of carbon dioxide in the ambient air. All experimental data sets were recorded in time intervals no greater than 2 h to minimize fluctuations in the compressed air stream. Finally, single-shot plasma temperature measurements were calculated from Boltzmann plots using 10 iron atomic emission lines in a single spectral window centered at 270 nm. The selected spectral lines were all Fe II emission lines, namely 258.588, 259.940, 261.187, 261.762, 271.441, 272.754, 273.955, 275.574, 277.93 and 278.369 nm. The upper energy levels ranged from 38 458 to 62 322  $\text{cm}^{-1}$ , thereby promoting precision due to the relatively broad spread of upper energy states. During the processing of single-shot spectra for temperature measurements, all spectra were first smoothed using the Savitzky–Golay algorithm [21,22].

## 3. Results and discussion

The primary goal of the present study is to assess the precision obtained during single-shot spectral analysis of LIBS data, noting any variability of precision with laser pulse energy. However, because pulse-to-pulse variability is significant at laser pulse energies near the break-

down threshold, noting the extreme case of non-breakdown, a careful study of the breakdown thresholds was performed first. The percentage of laser pulses producing breakdown was recorded as a function of laser pulse energy in the threshold range for laser-induced breakdown. Data were recorded for different gas stream conditions, including pure air, pure nitrogen, air with the introduction of deionized water at a mole fraction of 0.003, air with the introduction of titanium particles at a mass concentration of 17 ppm (mass), and air with the introduction of sodium particles at a mass concentration of 17 ppm. The mean particle diameters were approximately 25 nm, with corresponding aerosol number densities of approximately  $5 \times 10^8 \text{ cm}^{-3}$ . Defining a statistical breakdown threshold as the energy required to produce a 50% breakdown frequency, yielded a threshold energy ranging from 155 to 166 mJ over all gas stream conditions.

The pure gas streams are characterized by an abrupt breakdown threshold, changing from a breakdown percentage of less than 10% of laser shots at 160 mJ/pulse, to a breakdown percentage of approximately 90% at a pulse energy of 175 mJ. In contrast, the addition of solid particulates to the gas stream lowered the laser pulse energy required for breakdown, producing breakdown frequencies of approximately 20% at 80 mJ per pulse. The addition of water only mirrored the results of the solid particles, which is presumed due to the presence of submicron-sized water droplets acting as aerosols. The difference in the breakdown phenomena at low pulse energies between the purely gaseous and particle-laden streams is related to the generation of seed electrons during plasma initiation. Multiphoton ionization requires a well-defined photon flux for breakdown of nitrogen or oxygen, hence, the well-defined breakdown threshold in the gas streams. However, the presence of solid particles provides surface sites for multiphoton ionization, which though less photon-intensive than gas-phase breakdown, is a much less predictable process due to the complicated photon-particle surface interactions. It has been widely reported that the presence of fine particles greatly reduces the breakdown threshold [23–25]. For an estimated plasma volume diameter of 500  $\mu\text{m}$

(based on the measured laser beam diameter at the breakdown point), the 50% breakdown frequency corresponds to an average power density of approximately  $10 \text{ GW/cm}^2$ . A review of the literature for infrared irradiation ( $\sim 10$ -ns pulse width) reveals a broad variation in the breakdown threshold for clean air, ranging on the order of  $10^9$ – $10^{11} \text{ W/cm}^2$  [11,23,26,27]. For all experimental conditions in the present study, a breakdown frequency of 100% was realized at a pulse energy of 185 mJ. At this pulse energy, the incident photon flux is sufficiently high to uncouple the breakdown process from local matrix effects (e.g. aerosol loading), resulting in a repeatable, hence, robust plasma process. All subsequent experiments were performed at laser pulse energies between 185 and 350 mJ to ensure complete breakdown for all laser shots.

The energy deposited into the plasma, expressed as percentage of incident pulse energy, for purified air is shown in Fig. 1 as a function of the pulse energy. At a pulse energy of 192 mJ, which ensures 100% breakdown frequency, the plasma absorbs 48% of the incident pulse energy. Above this value, the percentage of absorbed energy increases steadily to a maximum value of approximately 60%, for pulse energies higher than approximately 250–260 mJ. This apparent saturation effect was observed first by Radziemski et al. [11], who reported a transmission of 5% (95% absorption) at 300 mJ, and later by Chen et al. [28] who obtained an absorption of 90% for incident energies from 45 to 80 mJ (13.4 mJ energy threshold,  $f/5$ , and 6.5-ns pulse width). Radziemski et al. explained that after sufficient energy is deposited in the plasma to ionize nearly all of the matter, the additional energy tends to expand the size of the plasma rather than increasing the temperature or electron density. The current experiments suggest a saturation pulse energy of approximately 255 mJ, with a corresponding energy density of  $2.1 \text{ kJ/cm}^3$ . This value is comparable to the energy density of  $5 \text{ kJ/cm}^3$  reported by Chen et al. [28].

The breakdown threshold and percentage of pulse energy deposited into the plasma should be considered in the context of two additional factors, namely spherical aberration and optical thickness. Parigger et al. conducted a theoretical study and

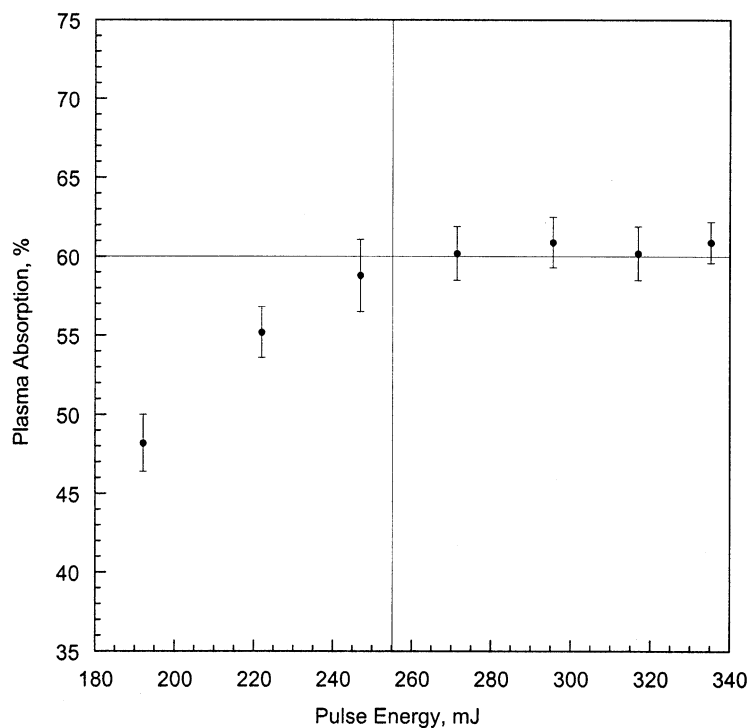


Fig. 1. Percentage of incident pulse energy absorbed by the laser-induced plasma as a function of laser pulse energy. Solid lines represent the apparent saturation value of 60% at a pulse energy of approximately 255 mJ. Error bars represent  $\pm 1$  S.D.

concluded that spherical aberration due to a single plano-convex lens with monochromatic light, reduces the irradiance at the focal spot by a factor of 10 from that obtainable in the absence of aberration [29]. In addition, spherical aberration can induce a large spot size with multiple breakdown sites along the optical axis, thereby increasing the transmission of energy and reducing overall absorption. Consequently, increased pulse energy is required to compensate for such an effect. Borghese et al. determined an average optical thickness of 0.8 in the plasma during the deposition of the second half of the incident pulse energy [30]. Using this value and the moving breakdown model by Docchio et al. [31], an estimated value of 66% for the absorption of pulse energy was calculated, in very good agreement with the current experimental value of 60%. The correlations between plasma characteristics and laser pulse energies, noting that saturation corresponds to

approximately 255 mJ, form the basis for the remainder of this paper.

The 247.8-nm carbon I atomic emission line was used for much of the current statistical analysis of the laser-induced plasma process. The source of carbon was carbon dioxide in the purified ambient air stream, which provided a homogeneous carbon source ( $\sim 100$  ppm of atomic carbon) at the molecular level. Such uniform dispersion of the analyte species is not readily achieved by the introduction of aerosol species. It is well known that the atomic emission signal strength of a given analyte species in a laser-induced plasma is a function of both laser pulse energy and of the temporal signal integration. To provide a valid comparison of carbon emission at different pulse energies, the carbon emission signal was optimized temporally for each different pulse energy, specifically using the ratio of the peak area of the carbon atomic line intensity (peak) to the average inten-

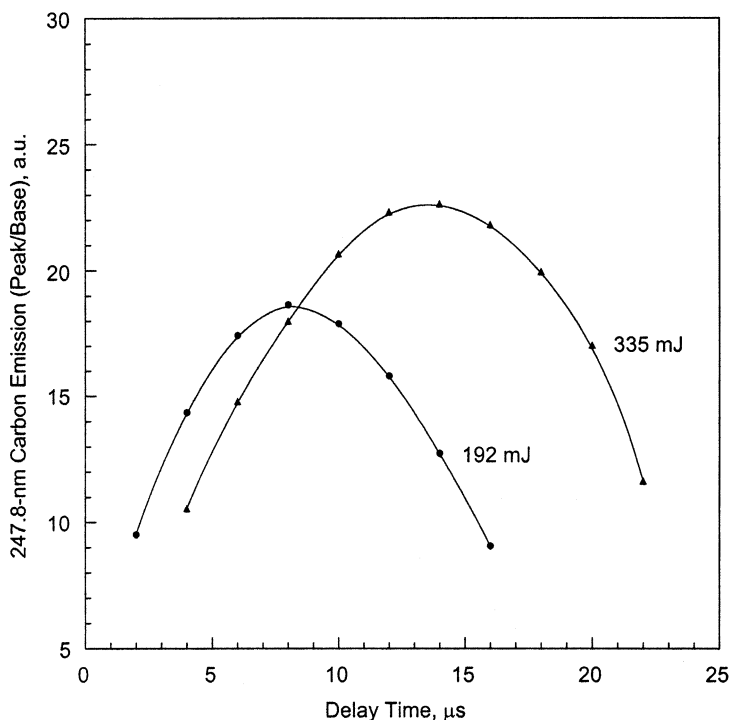


Fig. 2. Temporal optimization of the spectral carbon emission line (peak/base ratio) at 247.8 nm for two different laser pulse energies. A constant 2- $\mu$ s signal integration width was used for all data.

sity of the featureless continuum (base) near the atomic line, referred to as the peak-to-base ( $P/B$ ) ratio. Fig. 2 shows the LIBS signal response (peak/base) as a function of delay time with respect to the incident pulse for pulse energies of 192 and 335 mJ. The signal integration width was fixed at 2  $\mu$ s for all measurements. A similar trend is observed in both plots, namely a parabolic-like profile with a clear maximum. Such behavior has been widely reported, and is the result of differing rates of decay between the continuum and atomic emission processes. Similar plots were constructed for each of seven laser pulse energies used in this study. The data were used to construct a plot of the optimal delay time as a function of laser pulse energy. A second-order fit of the data enabled selection of the optimal delay time for each pulse energy, which was used for all subsequent experiments for the analysis of carbon. As discussed in detail below, the plasma temperature was found to be essentially constant (11 200 K) at each optimal

point, which is consistent with the plasma physics, whereby plasma temperature dictates the continuum emission and the populations of the various atomic transitions, hence, the  $P/B$  ratio.

Corresponding to the respective optimal delay times, the carbon atomic emission peak intensity and continuum base intensity, along with the corresponding peak-to-base ( $P/B$ ) and signal-to-noise ( $SNR$ ) ratios were measured as a function of pulse energy using an ensemble average of 100 spectra. All four parameters were found to increase with increasing pulse energy. When the pulse energy was increased from 200 to 344 mJ, the carbon emission peak and continuum intensity increased by 150 and 100%, respectively, while the carbon  $P/B$  and  $SNR$  increased by 20 and 60%, respectively. In addition, the rate of increase with pulse energy was not constant, but rather the parameters were characterized by a more marked increase up to pulse energies of approximately 250–275 mJ,

which coincides with the saturation effect discussed above.

While  $P/B$  and  $SNR$  ratios based on ensemble averages are widely used for optimization with LIBS-based analysis, the extension of the LIBS technique for single-shot analysis necessitates consideration of shot-to-shot fluctuations to enhance both accuracy and precision. The shot-to-shot variability over 100 laser pulses of the carbon emission peak, continuum intensity (base), and carbon emission peak-to-base ratio ( $P/B$ ) is examined in Fig. 3a for a pulse energy of 200 mJ, and in Fig. 3b for a pulse energy of 344 mJ. Several observations are made with respect to the two data sets. Careful inspection reveals a similar fluctuation pattern between the carbon atomic emission and continuum emission intensities. This scaling is observed in the  $P/B$  ratios, which vary by less than a factor of two between the maximum and minimum values in Fig. 3a, while the atomic emission and continuum values vary by more than a factor of six and four, respectively. Of greater significance, the fluctuations in the carbon emission peak, continuum emission, and  $P/B$  ratios are decreased with an increase in pulse energy. This is readily observed by comparing Fig. 3a and Fig. 3b. The relative standard deviation (R.S.D.) for the atomic emission and continuum emission intensities are 29 and 21%, respectively, at 200 mJ, and decrease to 11 and 9.5%, respectively, at 344 mJ. Similarly, the R.S.D. of the peak-to-base ratio decreased from a value of 11% at 200 mJ to 6% at 344 mJ. In addition to elucidating the effects of pulse energy on shot-to-shot precision, as discussed in detail below, these results demonstrate the usefulness of processing LIBS data based on the normalized peak-to-base ratio. While the atomic emission peak undergoes intense fluctuations, the normalized  $P/B$  ratio exhibits a significantly less variability, which is desirable for single-shot analysis.

In Fig. 4, the effect of laser pulse energy on the precision of the LIBS signal, as measured by both the  $P/B$  and the  $SNR$ , is illustrated. The relative standard deviation (R.S.D.) of both the carbon  $P/B$  and  $SNR$  values decreases with increasing laser pulse energy. Moreover, the rate of decrease from 200 to approximately 255 mJ was significantly

higher than for pulse energies in excess of 255 mJ. In fact, the R.S.D. of the peak-to-base values is essentially constant above 250 mJ. As presented above, pulse energy of approximately 255 mJ corresponds to the saturation value for absorption of pulse energy by the plasma. The results suggest a natural breakpoint at the saturation energy, resulting in a more repeatable, hence, more precise LIBS analyte signal for these laser pulse energies. As such, a greater robustness for quantitative single-shot LIBS measurements is realized after the plasma achieves a saturation condition.

To gain insight into the processes involved in the behavior discussed above, a series of single-shot plasma temperatures (based on Fe II emission) were calculated from individual spectra for varying laser pulse energies. Due to the high degree of signal noise associated with single-shot spectra, the individual spectra were sorted using a filtering algorithm to reject irregular spectra. Irregular spectra may arise from different sources, such as weak ionization of the plasma, a small amount of targeted analyte in the plasma volume, and the non-optimal collection of plasma emission. It is noted that iron was added in the form of an iron-based aerosol as described above, hence, the homogeneity of iron atoms is greatly reduced as compared to the gaseous carbon source. The weak ionization of the plasma can result from the absorption of laser energy by larger particles prior to reaching the focal spot; this induces a pre-breakdown that disrupts a normal energy-matter interaction at the nominal breakdown point. Because the analyte is derived from discrete iron particles, some plasma volumes may be characterized by weak analyte emission due to statistical fluctuations in the spatial distribution of iron particles. In the limiting case, no detectable quantity of the analyte may be present in a particular plasma. Using nominal values based on 1200-shot ensemble averages, a filtering algorithm was developed based on both absolute and relative intensities of the 259.9- and 258.58-nm, 272.75- and 271.44-nm, 277.93- and 271.44-nm, and the 278.36- and 271.44-nm iron II emission lines. The filtering algorithm resulted in the rejection of approximately 60–70% of the single-shot spectra. Nonetheless, the average plasma temperatures based on single-

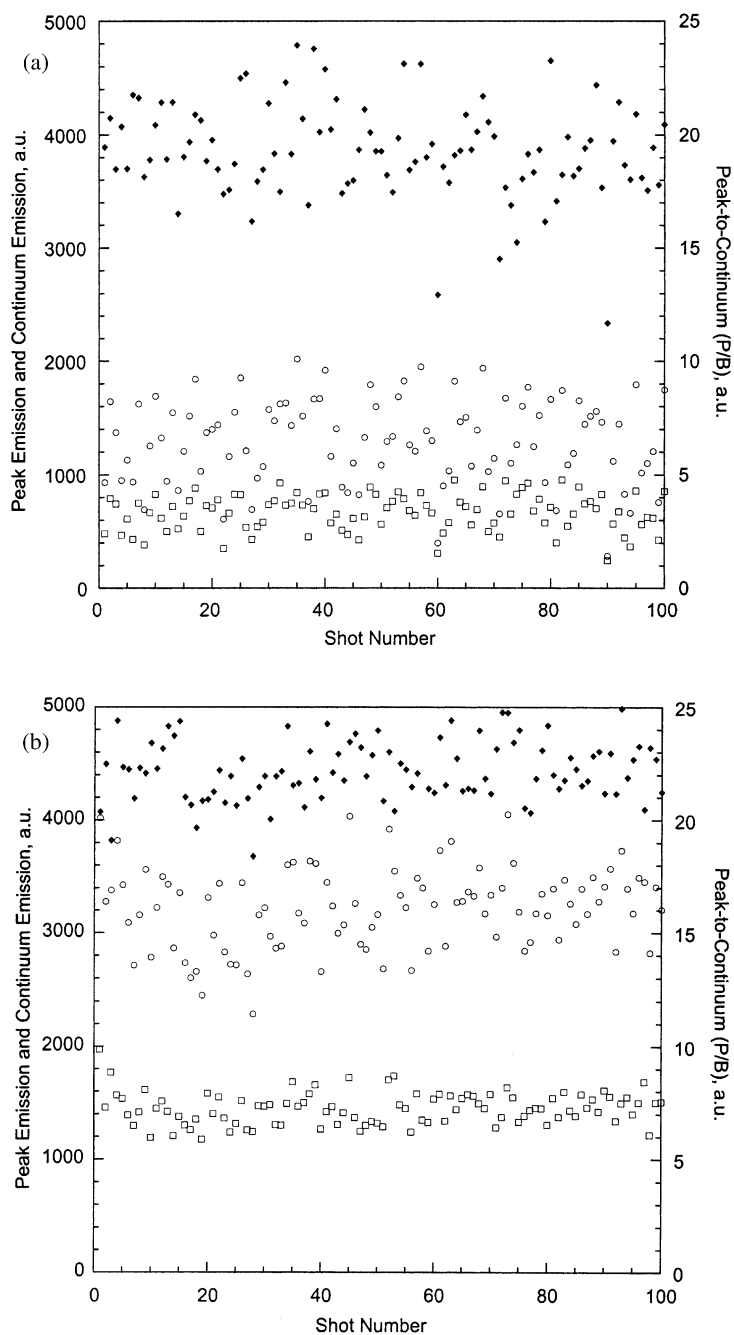


Fig. 3. Laser shot-to-shot variability of the peak emission (open circles), continuum emission (open squares), and peak/base ( $P/B$ ) ratio (solid diamonds) for the spectral carbon emission line at 247.8 nm for (a) 200-mJ laser pulse energy, and (b) 344-mJ laser pulse energy. Data correspond to the optimal time delay for each laser pulse energy. The peak signal has been scaled by a factor of 1/10.

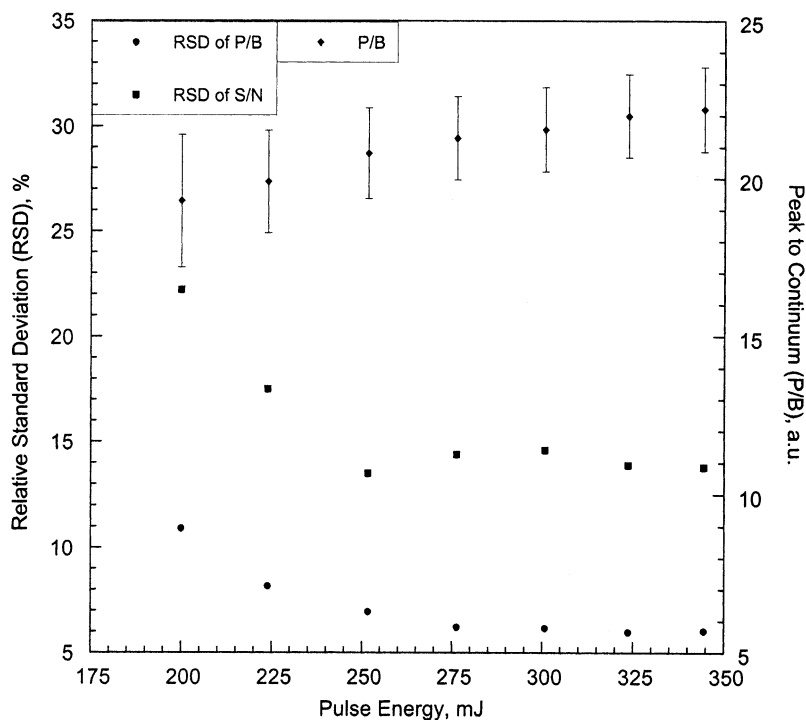


Fig. 4. Precision of the LIBS signal, expressed as the peak/base ( $P/B$ ) ratio and relative standard deviations (R.S.D.) of the peak/base ratio and signal/noise ( $S/N$ ) ratio, for the 247.8-nm carbon emission line as a function of laser pulse energy. Each data point represents the average of 100 single-shot calculations. Error bars represent  $\pm 1$  S.D.

shot measurements were in excellent agreement (within 10%) with plasma temperatures calculated directly from 1200-shot ensemble-averaged spectra, although a slight decrease in agreement was noted with increasing laser pulse energy.

The mean temperature and the corresponding R.S.D. based on 100 single-shot temperature measurements are presented in Fig. 5 as a function of the laser pulse energy. As can be observed from Fig. 5, the plasma temperature shows no significant change with increased laser pulse energy. Specifically, the highest and lowest plasma temperatures were 11 500 (11% R.S.D.) and 10 800 K (11% R.S.D.), with no statistical difference between these values. The average plasma temperature was 11 200 K (13% R.S.D.) for the seven laser pulse energies investigated. It is noted that the optimal delay time with respect to the carbon emission  $P/B$  ratio was used for each laser pulse energy. This supports the discussions above regarding temporal

optimization, namely that the envelope of optimal analyte emission lines for varying signal delays and laser pulse energies corresponds to the conditions of constant (i.e. optimal) plasma temperature for a given analyte.

A final observation regarding Fig. 5 is that the variability of the plasma temperature, based on the relative S.D.s, was found to be approximately constant as a function of laser pulse energy, with an average value of 12.8%. This stands in contrast with the behavior observed with the carbon emission parameters, which showed a marked decrease in variability with the onset of plasma saturation (see Fig. 4), as based on absorption of incident laser energy. This difference between shot-to-shot variations in atomic emission and plasma temperature offers insight into the overall precision of single-shot measurements. The temperature measurements make use of a Boltzmann plot, which depends on the relative intensities of the integrated

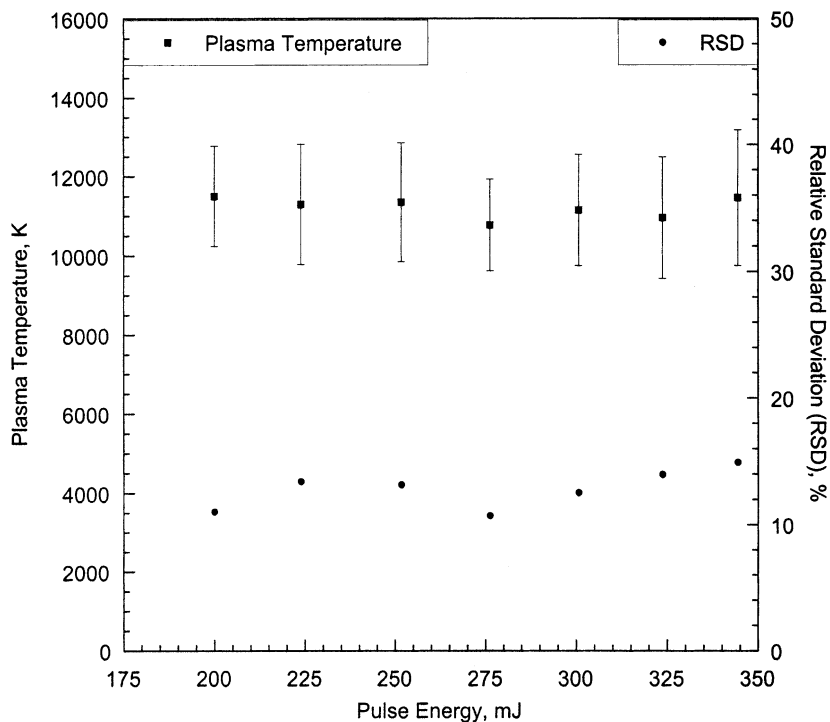


Fig. 5. Calculated plasma temperature and relative standard deviation (R.S.D.) of the plasma temperature as a function of laser pulse energy. Each data point is the average single-shot temperature calculations, and is based on iron II emission. Error bars represent  $\pm 1$  S.D.

iron atomic emission peaks. In contrast, quantitative analyte measurements (as reported in this paper) utilize atomic emission peak-to-base ratios, which depend on both the atomic emission and continuum emission signals. However, the actual emission signals (continuum and atomic) correspond to a spatial integration over the entire plasma, as coupled to the spectrometer/detector system using appropriate collection optics. The plasma itself is not completely homogeneous, and necessarily has property gradients due to boundary effects and its transient nature. Continuum emission and analyte atomic emission processes are non-linear processes; hence, it is fully expected that these two processes will differ relative to each other (i.e. peak-to-base ratios) throughout the plasma. In addition, theoretical description of the line-to-continuum ratio demonstrates the non-linear nature of this parameter with regard to plasma temperature, as discussed in a recent paper [29].

Accordingly, spatial variations in the position of the plasma will change the overall coupling of the plasma emission into the collection optics, thereby changing the effective spatial integration. Such changes are expected to be manifest in the resulting peak-to-base ratios. In contrast, atomic emission intensities of a specific analyte are expected to be more robust with respect to spatial integration simply because the coupling of two non-linear processes is avoided. Moreover, variations in absolute signal level are inconsequential for temperature measurements due to the logarithmic nature of the Boltzmann plot. While no quantitative measurements of plasma spatial stability were performed in the present study, it was readily observed that the plasma exhibited more variation in axial position at near-threshold pulse energies. It is further noted that the relative standard deviations of the shot-to-shot carbon  $P/B$  ratios and the iron-based plasma temperature values are essen-

tially equal (14.0 and 12.8%, respectively) in the saturation regime. Hence, these values may be interpreted as the inherent precision of the current LIBS system, encompassing intensifier and detector shot-noise as well as laser pulse energy stability. The additional variability (i.e. greater R.S.D.) realized at sub-saturation pulse energies most likely represents additional spatial variability, manifest through different plasma emission spatial integration as discussed above.

In concert, the current experiments lead to the suggestion that the reported decrease in plasma variability, hence enhanced precision, obtained in the plasma saturation regime, is due to a decrease in shot-to-shot spatial variability of the plasma. It is therefore concluded that single-shot LIBS based measurements should be made with sufficient laser pulse energy to achieve saturation with respect to absorbed pulse energy, as well as made with a suitable collection geometry (e.g. backscatter mode) to minimize spatial variability.

## Acknowledgments

This work was supported in part by the US Department of Energy in conjunction with Sandia National Laboratories, Livermore, California, and in part by the Engineering Research Center for Particle Science and Technology at the University of Florida.

## References

- [1] U.S. Environmental Protection Agency, Federal Register 61 (77) (1996) 17357–17358.
- [2] H. Zhang, F.Y. Yueh, J.P. Singh, Laser-induced breakdown spectrometry as a multimetal continuous-emission monitor, *Appl. Opt.* 38 (1999) 1459–1466.
- [3] R.E. Neuhauser, U. Panne, R. Niessner, P. Wilbring, On-line monitoring of chromium aerosol in industrial exhaust streams by laser-induced plasma spectroscopy (LIPS), *Fresenius J. Anal. Chem.* 364 (1999) 720–726.
- [4] R.E. Neuhauser, U. Panne, R. Niessner, G.A. Petrucci, P. Cavalli, N. Omenetto, On-line and in-situ detection of lead aerosols by plasma-spectroscopy and laser-excited atomic fluorescence spectroscopy, *Anal. Chim. Acta* 346 (1997) 37–48.
- [5] K. Song, Y.-I. Lee, J. Sneddon, Applications of laser-induced breakdown spectrometry, *Appl. Spectrosc. Rev.* 32 (1997) 183–235.
- [6] J. Sneddon, Y.-I. Lee, Novel and recent applications of elemental determination by laser-induced breakdown spectrometry, *Anal. Lett.* 32 (1999) 2143–2162.
- [7] D.A. Rusak, B.C. Castle, B.W. Smith, J.D. Winefordner, Fundamentals and applications of laser-induced breakdown spectroscopy, *Crit. Rev. Anal. Chem.* 27 (1997) 257–290.
- [8] D.W. Hahn, Laser-induced breakdown spectroscopy for sizing and elemental analysis of discrete aerosol particles, *Appl. Phys. Lett.* 72 (1998) 2960–2962.
- [9] D.W. Hahn, M.M. Lunden, Detection and analysis of aerosol particles by laser-induced breakdown spectroscopy, *Aerosol Sci. Technol.* 33 (2000) 30–48.
- [10] J.E. Carranza, B.T. Fisher, G.D. Yoder, D.W. Hahn, On-line analysis of ambient air aerosols using laser-induced breakdown spectroscopy, *Spectrochim. Acta Part B* 56 (2001) 851–864.
- [11] L.J. Radziemski, T.R. Loree, D.A. Cremers, N.M. Hoffman, Time-resolved laser-induced breakdown spectrometry of aerosols, *Anal. Chem.* 55 (1983) 1246–1252.
- [12] S. Yalcin, D.R. Crosley, G.P. Smith, G.W. Faris, Spectroscopic characterization of laser-produced plasmas for in situ toxic metal monitoring, *Hazard. Waste Hazard. Mater.* 13 (1996) 51–61.
- [13] R.L. Gleason, D.W. Hahn, The effects of oxygen on the detection of mercury using laser-induced breakdown spectroscopy, *Spectrochim. Acta Part B* 56 (2001) 419–430.
- [14] I. Schechter, Direct aerosol analysis by time resolved laser plasma spectroscopy. Improvement by single shot measurements, *Anal. Sci. Technol.* 8 (1995) 779–786.
- [15] L. Xu, V. Bulatov, V.V. Gridin, I. Schechter, Absolute analysis of particulate materials by laser-induced breakdown spectroscopy, *Anal. Chem.* 69 (1997) 2103–2108.
- [16] I.B. Gornushkin, B.W. Smith, G.E. Potts, N. Omenetto, J.D. Winefordner, Some considerations on the correlation between signal and background in laser-induced breakdown spectroscopy using single-shot analysis, *Anal. Chem.* 71 (1999) 5447–5449.
- [17] D.W. Hahn, W.L. Flower, K.R. Hencken, Discrete particle detection and metal emissions monitoring using laser-induced breakdown spectroscopy, *Appl. Spectrosc.* 51 (1997) 1836–1844.
- [18] M.D. Cheng, Real-time measurement of trace metals on fine particles by laser-induced plasma techniques, *Fuel Process. Technol.* 65–66 (2000) 219–229.
- [19] B.C. Castle, K. Talabardon, B.W. Smith, J.D. Winefordner, Variables influencing the precision of laser-induced breakdown spectroscopy measurements, *Appl. Spectrosc.* 52 (1998) 649–657.
- [20] D.W. Hahn, J.E. Carranza, G.R. Arsenault, H.A. Johnsen, K.R. Hencken, Aerosol generation system for development and calibration of laser-induced breakdown spectroscopy instrumentation, *Rev. Sci. Instrum.* 72 (2001) 3706–3713.
- [21] H.H. Madden, Comments on the Savitzky–Golay convolution method for least-square fit smoothing and

- differentiation of digital data, *Anal. Chem.* 50 (1978) 1383–1386.
- [22] A. Savitzky, M.J.E. Golay, Smoothing and differentiation of data by simplified least squares procedures, *Anal. Chem.* 36 (1964) 1627–1639.
- [23] D.C. Smith, Gas-breakdown initiated by laser-radiation interaction with aerosols and solid-surfaces, *J. Appl. Phys.* 48 (1977) 2217–2225.
- [24] D.E. Lencioni, L.C. Pettingill, Dynamics of air breakdown initiated by a particle in a laser-beam, *J. Appl. Phys.* 48 (1977) 1848–1851.
- [25] A.A. Lushnikov, A.E. Negin, Aerosols in strong laser-beams, *J. Aerosol Sci.* 24 (1993) 707–735.
- [26] R.A. Armstrong, R.A. Lucht, W.T. Rawlins, Spectroscopic investigation of laser-initiated low-pressure plasmas in atmospheric gases, *Appl. Optics* 22 (1983) 1573–1577.
- [27] J.B. Simeonsson, A.W. Miziolek, Spectroscopic studies of laser-produced plasmas formed in CO and CO<sub>2</sub> using 193-, 266-, 355-, 532- and 1064-nm laser-radiation, *Appl. Phys. B* B59 (1994) 1–9.
- [28] Y.L. Chen, J.W.L. Lewis, C. Parigger, Spatial and temporal profiles of pulsed laser-induced air plasma emissions, *J. Quant. Spectrosc. Radiat. Transfer* 67 (2000) 91–103.
- [29] C. Parigger, Y. Tang, D.H. Plemmons, J.W.L. Lewis, Spherical aberration effects in lens-axicon doublets: theoretical study, *Appl. Opt.* 36 (1997) 8214–8221.
- [30] A. Borghese, S.S. Merola, Time-resolved spectral and spatial description of laser-induced breakdown in air as a pulsed, bright, and broadband ultraviolet-visible light source, *Appl. Opt.* 37 (1998) 3977–3983.
- [31] F. Docchio, P. Regondi, M.R.C. Capon, J. Mellerio, Study of the temporal and spatial dynamics of plasmas induced in liquids by nanosecond Nd:YAG laser pulses. I: Analysis of the plasma starting times, *Appl. Opt.* 27 (1988) 3661–3668.